

A Redshift Determination for XRF 020903: First Spectroscopic Observations of an X-ray Flash

A. M. Soderberg, S. R. Kulkami, E. Berger, D. B. Fox, P. A. Price, S. Yost and M. Hunt
Division of Physics, Mathematics and Astronomy, M/S 105-24, California Institute of
Technology, Pasadena, CA 91125

D. A. Frail and C. Walker

National Radio Astronomy Observatory, P.O. Box 0, Socorro, NM 87801

M. Hamuy and S. Shectman

Carnegie Observatories, 813 Santa Barbara Street, Pasadena, CA 91101

and

J. Halpern and N. M. Trabal

Astronomy Department, Mailcode 5246, Columbia University, New York, NY 10027

ABSTRACT

We report the discovery of optical and radio afterglow emission from the extremely soft X-ray flash, XRF 020903. Our spectroscopic observations provide the first redshift for an X-ray flash, thereby setting the distance scale for these events. At $z = 0.251$, XRF 020903 is one of the nearest cosmological explosions ever detected, second only to the recent GRB 030329 and the unusual GRB 980425/SN 1998bw. Moreover, XRF 020903 is the first X-ray flash for which we detect an optical afterglow. The luminosity of the radio afterglow of XRF 020903 is 1000 times greater than that of Ibc supernovae but similar to those of GRB afterglows. From broadband afterglow modeling we show that the explosion energy of XRF 020903 is not dissimilar from values inferred for typical gamma-ray bursts, suggesting that these cosmological explosions may derive from a similar mechanism.

Subject headings: gamma-ray bursts: specific (XRF 020903) | supernovae: general

1. Introduction

Prior to the detection of afterglows, gamma-ray bursts (GRBs) were enshrouded in mystery for nearly thirty years. Great progress in our understanding of these energetic events came with the first redshift measurement which placed GRBs at cosmological distances (Metzger et al. 1997). In a similar fashion, the mystery of X-ray flashes (XRFs) has been fueled by the absence of confirmed redshifts. These events, identified in the 1990's by BeppoSAX, are characterized by a peak energy in F of $E_{\text{peak}} = 25 \text{ keV}$ (compared to $E_{\text{peak}} = 250 \text{ keV}$ for GRBs). With a distribution of durations similar to those observed for GRBs, it has been assumed that XRFs are associated with GRBs and therefore share their extragalactic distance scale (Heise et al. 2001).

The subsequent discovery of XRF X-ray and radio afterglows with properties similar to those observed in GRB afterglows has further strengthened this association (Harrison et al. 2001; Amati et al. 2002; Taylor, Frail & Kulkami 2001). Still, the question of whether the difference between GRBs and XRFs is intrinsic or extrinsic remains unanswered. Assuming XRFs are simply GRBs observed away from the jet collimation axis, they would have less X-ray emission and the difference is extrinsic, based solely on the line-of-sight to the observer. On the other hand, the difference could be intrinsic, namely XRFs may represent a class of explosions which are similar in energetics to GRBs yet characterized by less relativistic ejecta possibly due to a heavier baryonic load. It is clear that by setting the distance scale for XRFs (and hence their energy scale) we can begin to distinguish between extrinsic and intrinsic effects.

In this paper we present the first spectroscopic redshift for an X-ray ash, XRF 020903, placing this event among the nearest high energy explosions and offering confirmation that X-ray flashes are cosmological and produce a total energy output similar to that observed in GRBs.

2. Observations

On 2002 September 3.421 UT the Wide-Field X-ray Monitor (WXM) and Soft X-ray Camera (SXC) aboard the High Energy Transient Explorer-2 (HETE-2) detected an X-ray ash within the 0.5-10 keV energy band. With an exceptionally low peak energy of $E_{\text{peak}} = 5 \text{ keV}$ and a fluence of $7.2 \times 10^{-8} \text{ erg cm}^{-2}$, XRF 020903 is the softest event ever detected by HETE-2 with a ratio of X-ray fluence (S_X) to X-ray fluence (S) of $\log(S_X/S) = 4.3$ (Sakamoto et al. 2003). Ground analysis provided a localization for XRF 020903 centered at $(J2000) = 22^{\text{h}}49^{\text{m}}01^{\text{s}}$, $(J2000) = 20^{\circ}55'47''$ with a $4^{\circ} \times 31^{\circ}$ uncertainty region at $t = 0.3$

days (Ricker et al. 2002).

2.1. Ground-based Photometry

We began observing the field of XRF 020903 on 2002 September 4.32 UT ($t = 0.9$ days) with the Palomar Observatory 200-inch telescope (P200) equipped with the Large Field Camera (LFC). With a total exposure time of 20 minutes under photometric conditions (stellar FWHM = $1.2^{\text{''}}$) the observations reached a limiting magnitude of $R = 23$ mag. Visual comparison with Digitized Sky Survey archival images did not reveal an afterglow candidate.

A second epoch was obtained on September 10.30 UT ($t = 7$ days) using the same observational set-up and in similar observing conditions. Image subtraction between the first and second epochs revealed one variable object within the HETE-2 error region (Figure 1) located at $(\text{J2000}) = 22^{\text{h}}48^{\text{m}}42.34^{\text{s}}$, $(\text{J2000}) = 20^{\circ}46'09.3^{\text{''}}$ and lying 4 arcsec NW of a bright elliptical galaxy (hereafter G2; Soderberg et al. 2002).

With an approximate magnitude of $R = 19$ at $t = 1$ day, the new object decreased in brightness by 1.4 magnitudes between the two epochs, implying a temporal flux decay index of -1.1 . As the source proved consistent with a typical GRB afterglow evolution, the optical transient was adopted as a suitable candidate for the optical afterglow of XRF 020903.

We observed the afterglow position on three additional epochs with the P200 and the McDonald Observatory 1.3-meter telescope (Table 1). These, along with Digitized Sky Survey archival images, reveal the presence of an extended source with $R = 21$ mag coincident with the position of the transient and thereby suggestive of a host galaxy (hereafter G1).

Due to the underlying extended source and the proximity of the transient to G2, accurate magnitude estimates relied on careful PSF photometry of the field. Absolute calibration of field stars was supplied by Henden (2002). We used 12 unsaturated field stars in common between the Palomar and Henden images to fully calibrate observations of the variable source. We note that although the transient decreased in brightness quickly between the first two epochs, later epochs ($t = 30 - 40$ days) appear to indicate a plateau in the light curve which was confirmed by other observers (Gorosabel et al. 2002) and may originate from unresolved flux contamination from G1.

2.2. Ground-based Spectroscopy

Initial spectroscopy of the transient was performed on 2002 September 28.1 UT with the Magellan Baade Telescope using the Low Dispersion Survey Spectrograph (LDSS2). A position angle of 168 degrees was used such that spectral information on G1 and G2 was obtained simultaneously. Despite the positional coincidence of G2 and G1, it was found that the systems are not physically associated, separated by 3900 km/s in velocity space (Soderberg et al. 2002). In this epoch, the transient source was still significantly bright.

Further spectroscopic observations were made of the putative host (G1) with the Echelle Spectrograph & Imager (ESI) mounted on the Keck II telescope on 2003 July 4 UT ($t = 300$ days). These observations do not include any flux from the transient source. During a total exposure time of 1 hour, we obtained a spectrum of G1 and G2 with a slit width of 0.75 arcsec.

We find that G2 is a large elliptical galaxy with at least one interacting galaxy companion, G3, located $< 1''$ to the NE (see Figure 3). Observations of G2 exhibit a relatively smooth continuum with features typical of an elliptical galaxy. The Ca II H and K absorption lines give a redshift of $z = 0.235$, while G3 is offset by only 240 km/s at a redshift of $z = 0.236$.

In contrast, G1 is shown to be an active star-forming galaxy at $z = 0.251$ with a rich set of narrow bright emission lines (Figure 2). The [O III]/H and [N II]/H intensity ratios indicate that the galaxy is a low-metallicity and high-excitation starburst galaxy. In addition, the flux ratio of the [Ne III] and [O II] lines is $F^{3869} = F^{3727} = 0.43$, similar to the observed value for the host galaxy of GRB 970508 (Bloom et al. 1998) and approximately 10 times higher than typical values for H II regions. The bright [Ne III] emission lines observed in GRB hosts are thought to be indicative of a substantial population of massive stars. On the other hand, Chornock & Filippenko (2002) note that a spectrum of G1 taken with the Low Resolution Imaging Spectrometer (LRIS) on the Keck I telescope reveals a deficit of emission at rest wavelengths $< 4000\text{\AA}$ which is consistent with a population of older stars.

2.3. Hubble Space Telescope

The afterglow candidate was observed with the Hubble Space Telescope (HST) using the Advanced Camera for Surveys (ACS) under Program No. 9405 (P.I.: A. Fruchter). Three epochs of imaging were obtained from $t = 94$ to 300 days with exposure times of 1840 sec in the F606W filter. Following "On-The-Fly" pre-processing the data were drizzled using standard IRAF tools (STSDAS; Fruchter & Hook 2002). In drizzling our final images, we

retained the native WFC pixel scale of 0.05" and used a pixfrac of 1.0. The HST images reveal a complex galaxy morphology for G1, suggesting a system of at least four interacting galaxies (see Figure 3).

To locate the optical transient with respect to the host galaxy complex, we performed a source to source comparison of our first-epoch Palomar (2002 September 4) and HST (2002 December 3) images. We found 42 unsaturated, unconfused sources in common between these two images, and were able to match the two coordinate lists with an rms mapping uncertainty of 0.06 arcsec. We derived the position of the transient from the difference in age of the 2002 September 4 and September 10 data. Since the optical transient is well-detected in the difference in age, the uncertainty in its centroid position is negligible. The uncertainty in the coordinate mapping thus dominates the uncertainty in the position of the source relative to the host galaxy complex. The optical transient appears to overlap with the SW component of the G1 complex (Figure 3).

2.4. Radio Observations of XRF 020903

2.4.1. Very Large Array Data

We began observations of the field of XRF 020903 with the Very Large Array (VLA¹) on 2002 September 27 22 UT. A radio source was detected in coincidence with the optical transient at a location of $(J2000) = 22^{\text{h}}48^{\text{m}}42.34^{\text{s}}$; $(J2000) = 20^{\circ}46'08.9''$ with an uncertainty of 0.1 arcsec in each coordinate. The initial observation showed the radio source to have a flux density of $F = 1.06 \pm 0.02$ mJy at 8.5 GHz. The National Radio Astronomy Observatory VLA Sky Survey (NVSS; Condon et al. 1998) did not show any evidence for a pre-existing source at this location down to a limit of 1 mJy. Further observations at 8.5 GHz on September 29.11 (at 26 days) showed that the source faded to $F = 0.75 \pm 0.04$ mJy. We continued monitoring the transient source with the VLA over the next 370 days at frequencies of 1.5, 4.9, 8.5 and 22.5 GHz. The lightcurve is displayed in Figure 4.

2.4.2. Very Long Baseline Array Data

The relatively low redshift and strong radio emission of the transient source made it an ideal candidate for Very Long Baseline Array (VLBA) observations. On September 30.23

¹The VLA is operated by the National Radio Astronomy Observatory, a facility of the National Science Foundation operated under cooperative agreement by Associated Universities, Inc.

UT ($t = 27$ days) we observed the radio transient for a total duration of 6 hours at 8.5 GHz. Using sources J2253+1608 and J2148+0657 we were able to flux calibrate the field and we phase referenced against source J2256-2011 at a distance of < 2 degrees. Data were reduced and processed using standard VLBA packages within the Astronomical Image Processing System (AIPS). We detected the radio transient with a flux of 0.89 ± 0.17 mJy at a position coincident with the VLA and optical observations at a location of (J2000) = $22^h 48^m 42.33912^s$ 0.00003 , (J2000) = $20^{\circ} 46' 08.945^{\circ}$ 0.0005 . This is our most accurate position measurement for the transient object. The source is unresolved within our VLBA beam size of 1.93 ± 1.73 mas. Furthermore, the consistency between the flux measured with VLBA and low resolution VLA observations rules out the presence of diffuse components (e.g. jets).

3. The afterglow of XRF 020903

The large error box and the proximity of the optical transient to G 2 and G 3 delayed rapid identification of the transient (Price, Schmidt & Axelrod 2002; Pavlenko, Rumyantsev & Pozanenko 2002; Uemura et al. 2002; Fruchter et al. 2002). As a result there was little optical follow up of the transient at early times (see Table 1). At later times, the transient is rapidly dominated by the emission from G 1. An additional complication was introduced by Gal-Yam (2002) who, based on archival photographic plates from 1954 and 1977, proposed that G 1 hosted an active galactic nuclei (AGN) which was time variable.

In contrast to the above discussion, the extensive radio light curve (Figure 4) provides strong evidence that the transient is the afterglow of XRF 020903. The radio light curve is similar to the afterglow of GRBs (Frail et al. 2003). At 4.9 GHz, the source was observed to rise to a peak flux at $t = 29$ days and subsequently decay with a characteristic index of -1.1 . A steeper decline of $F \propto t^{-1.5}$ was observed at 8.5 GHz where the peak flux precedes the first observational epoch. We note that the dynamical range of the radio afterglow emission clearly distinguishes the source from a radio bright AGN.

The afterglow interpretation is consistent with the optical spectroscopic observations of G 1, namely the absence of broad lines or line features typical of AGN as well as the absence of any jet structure in the VLBA images of the radio transient. We now proceed accepting the notion that the optical/radio transient is the afterglow of XRF 020903.

4. Energetics

At a redshift of $z = 0.251$, the X-ray fluence implies an isotropic equivalent energy $E_{\text{iso}} = 1.1 \times 10^{49}$ erg. This value is 3 to 6 orders of magnitude lower than the isotropic energies of gamma-ray bursts (Frail et al. 2001). Since there is no evidence for a jet break in the afterglow observations, the data are consistent with a wide jet or a spherical explosion.

Figure 5 shows that although the energy in the prompt emission of XRF 020903 is significantly lower than that observed for typical GRBs, the peak luminosity of the radio afterglow is comparable to that found in GRB afterglows. This indicates that XRF 020903 has a similar kinetic energy to GRB afterglows. To study this in more detail we used standard broadband afterglow models with spherical and collimated ejecta expanding into circumburst media with uniform density and wind density profile, $\rho \propto r^{-2}$ (Berger et al. 2000). We find that independent of the assumed model, the total kinetic energy is $E = 4 \times 10^{50}$ erg with reasonable values for the circumburst density and energy fractions (electron and magnetic field) of $n = 100 \text{ cm}^{-3}$, $e = 0.6$ and $B = 0.01$, respectively. Thus we confirm the afterglow energy is similar to values found for GRB afterglows (Panaitescu & Kumar 2002; Berger, Kulkami & Frail 2003).

Recent evidence suggests a standard total energy yield (10^{51} erg) for all GRBs, where the total energy yield (E_{tot}) is defined as the sum of the energy in the prompt emission (E_{p}) plus the mildly relativistic energy as inferred from the afterglow (E_{rad}), such that $E_{\text{tot}} = E_{\text{p}} + E_{\text{rad}}$ (Berger et al. 2003b). Clearly, for XRF 020903 the explosion energy is dominated by the mildly relativistic afterglow, while less energy couples to the high Lorentz factors characterizing the prompt emission.

Figure 5 also compares the radio luminosity of XRF 020903 with other spherical explosions (type Ibc supernovae). With a radio luminosity 1000 times greater than typical Ibc SNe, it is clear that XRF 020903 is a significantly more energetic explosion. This suggests that despite their similar explosion geometries, XRF 020903 and type Ibc supernovae are intrinsically different (possibly due to the presence of a central engine (Berger et al. 2003a)).

5. Conclusions

We present radio and optical observations of the afterglow of XRF 020903 (the first X-ray flash to have a detected optical afterglow and a spectroscopic distance determination). At a redshift of $z = 0.251$, this burst has set the distance scale for XRFs and confirmed the assumption they are cosmological in origin. The host galaxy of XRF 020903 appears to be a typical star-forming galaxy similar to those of GRB host galaxies.

The isotropic energy release of the prompt (X-ray) emission of XRF 020903 is at least two orders of magnitude smaller than those of GRBs. However, from our broadband modeling of the afterglow we determine that the total kinetic energy is about 10^{50} erg, not dissimilar to those inferred for GRBs (Frailey et al. 2001; Berger, Kulkami & Frail 2003). In comparison with a larger sample of cosmic explosions, XRF 020903 is a clear example where less energy is coupled to high Lorentz factors. This source highlights the diversity in high energy transients and underscores the importance of studying spherical explosions.

AM S is supported by an NSF graduate fellowship. GRB research at Caltech is supported by NASA and NSF.

REFERENCES

Amati, L., Capalbi, M., Frontera, F., Gandolfo, G., Piro, L., 't Zand, J. J. M., Granata, S., and Reali, F. 2002, GRB Circular Network, 1386, 1.

Berger, E., Kulkami, S. R., and Frail, D. A. 2003, ApJ, 590, 379.

Berger, E., Kulkami, S. R., Frail, D. A., and Soderberg, A. M. 2003a, Accepted to ApJ, astro-ph/0307228.

Berger, E. et al. 2003b, Accepted to Nature, astro-ph/0308187.

Berger, E. et al. 2000, ApJ, 545, 56.

Bloom, J. S., Djorgovski, S. G., Kulkami, S. R., and Frail, D. A. 1998, ApJ, 507, L25.

Chomiuk, R. and Filippenko, A. V. 2002, GRB Circular Network, 1609, 1.

Condon, J. J., Cotton, W. D., Greene, E. W., Yin, Q. F., Perley, R. A., Taylor, G. B., and Broderick, J. J. 1998, AJ, 115, 1693.

Frail, D. A., Kulkami, S. R., Berger, E., and Wieringa, M. H. 2003, AJ, 125, 2299.

Frail, D. A. et al. 2001, ApJ, 562, L55.

Fruchter, A., Strolger, L., Mobasher, B., Rhoads, J., Levan, A., Burud, I., and Becker, A. 2002, GRB Circular Network, 1557, 1.

Fruchter, A. S. and Hook, R. N. 2002, PASP, 114, 144.

Gal-Yam, A. 2002, GRB Circular Network, 1556, 1.

Gorosabel, J., Hjorth, J., Pedersen, H., Jensen, B. L., Fynbo, J. P. U., Andersen, M., Castro Cerón, J. M., and Castro-Tirado, A. J. 2002, *GRB Circular Network*, 1631, 1.

Harrison, F. A., Yost, S., Fox, D., Heise, J., Kulkami, S. R., Price, P. A., and Berger, E. 2001, *GRB Circular Network*, 1143, 1.

Heise, J., in't Zand, J., Kippen, R. M., and Woods, P. M. 2001, in *Gamma-ray Bursts in the Afterglow Era*, 16.

Henden, A. 2002, *GRB Circular Network*, 1571, 1.

Metzger, M. R., Djorgovski, S. G., Kulkami, S. R., Steidel, C. C., Adelberger, K. L., Frail, D. A., Costa, E., and Frontera, F. 1997, *Nature*, 387, 878.

Panaitescu, A. and Kumar, P. 2002, *ApJ*, 571, 779.

Pavlenko, E., Rumyantsev, V., and Pozanenko, A. 2002, *GRB Circular Network*, 1535, 1.

Price, P. A., Schmidt, B. P., and Axelrod, T. S. 2002, *GRB Circular Network*, 1533, 1.

Ricker, G. et al. 2002, *GRB Circular Network*, 1530, 1.

Sakamoto, T. et al. 2003, Submitted to *ApJ*, astro-ph/0309455.

Soderberg, A. M. et al. 2002, *GRB Circular Network*, 1554, 1.

Taylor, G. B., Frail, D. A., and Kulkami, S. R. 2001, *GRB Circular Network*, 1136, 1.

Uemura, M., Ishioka, R., Kato, T., and Yamamoto, H. 2002, *GRB Circular Network*, 1537, 1.

Yun, M. S. and Carilli, C. L. 2002, *ApJ*, 568, 88.

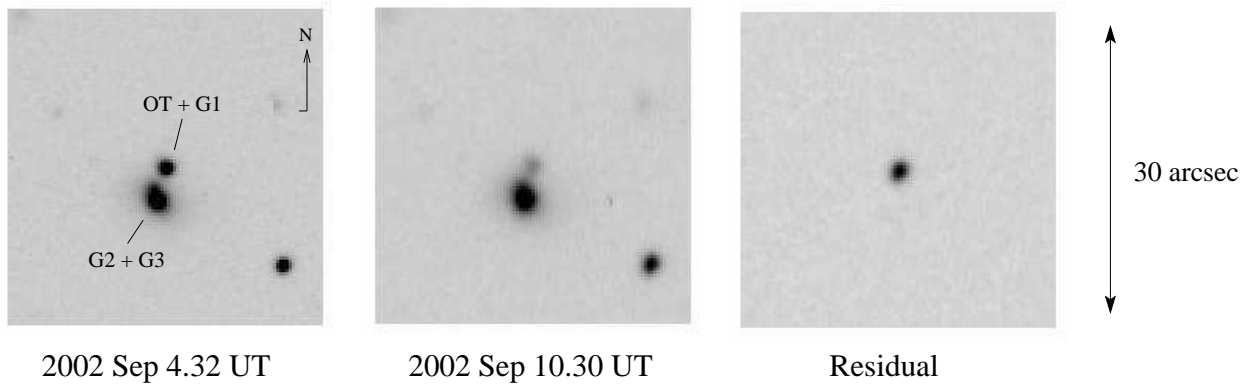


Fig. 1. The field of XRF 020903 was observed with the Palomar 200 inch telescope equipped with the Large Field Camera on 2002 September 4.32 and September 10.30 UT. Image subtraction techniques revealed one variable object within the HETE-2 error-box lying 4 arcsec NW of a bright elliptical galaxy (G 2). The residual image clearly indicates a transient stellar source which decreased in brightness by 1.4 magnitudes between the two epochs.

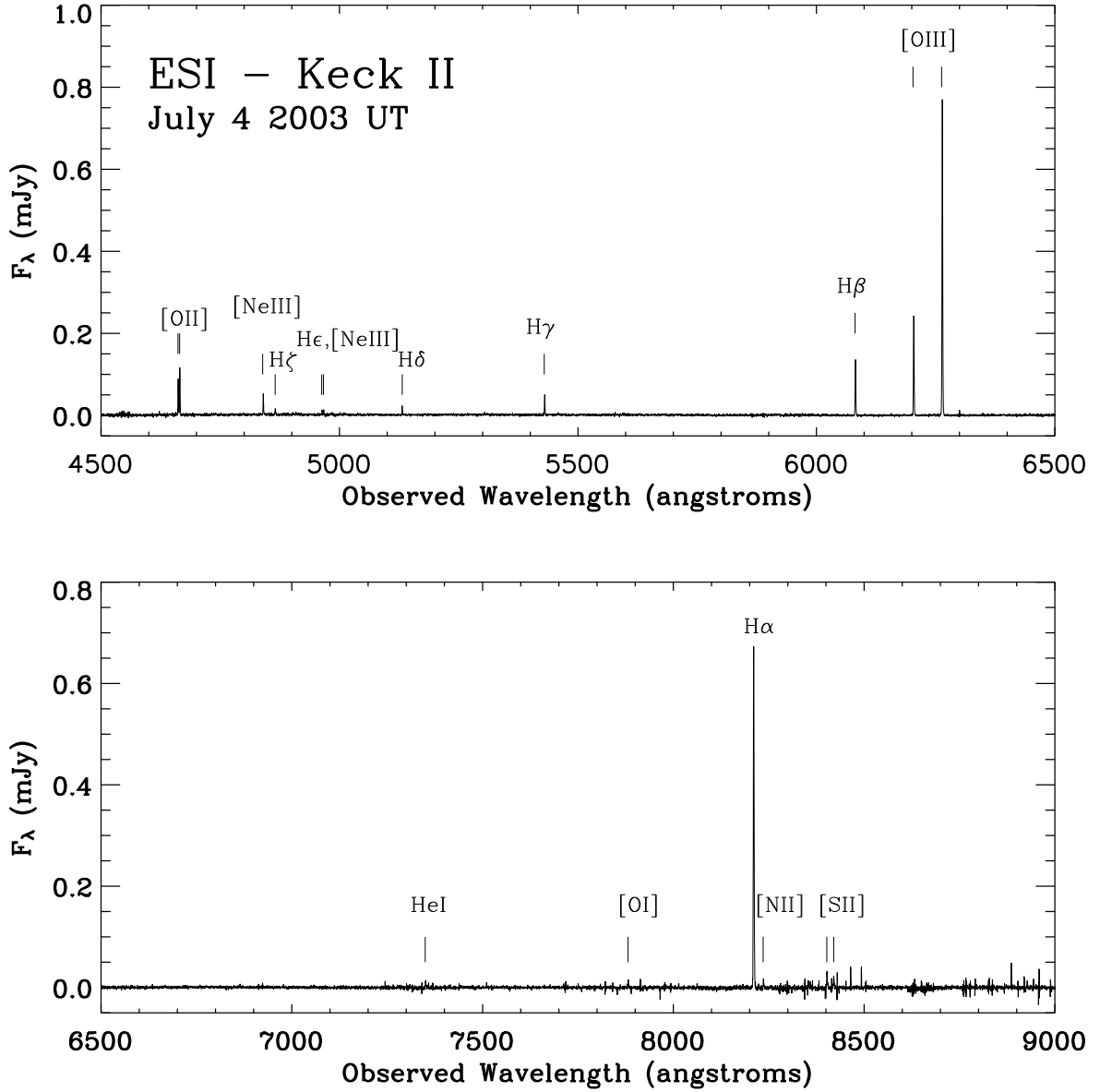


Fig. 2. On 2003 July 4 UT we obtained spectroscopic observations of the putative host galaxy (G 1) underlying the optical transient source associated with XRF 020903. Data were taken with the Echelle Spectroscopic Imager (ESI) mounted on the Keck II telescope. The source is shown to be an active star-forming galaxy at $z=0.251$ with a rich set of narrow bright emission lines.

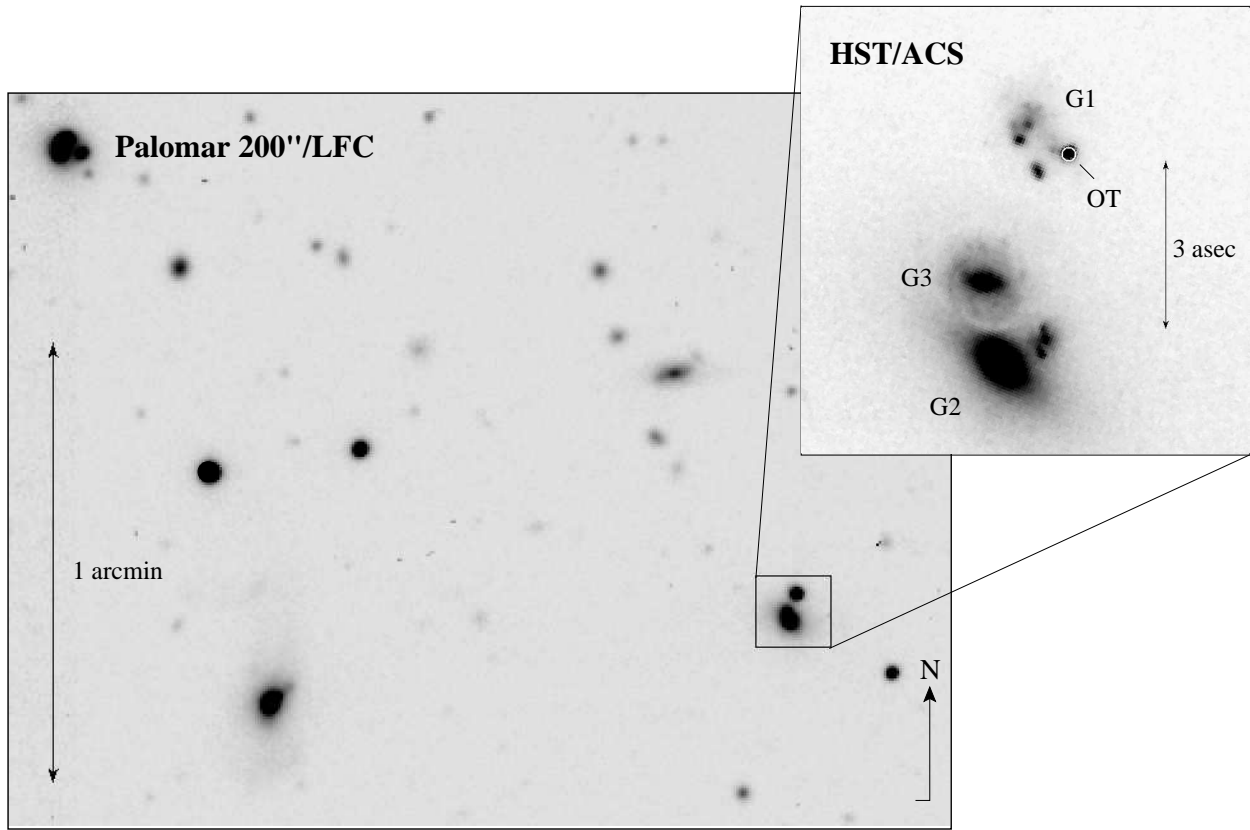


Fig. 3. The transient discovered within the error box of XRF 020903 was observed with the Hubble Space Telescope (HST) using the Advanced Camera for Surveys (ACS) on 2002 December 3 UT. The HST image reveals a complicated galaxy morphology for G 1, suggesting a system of at least four interacting galaxies. The location of the optical transient is noted on the $7''$ HST cutout with a circle which represents a 2 σ positional uncertainty of $0.12''$. Nearby galaxies G 2 and G 3 are labeled accordingly on the HST image. The optical transient appears to overlap with the SW component of the G 1 complex.

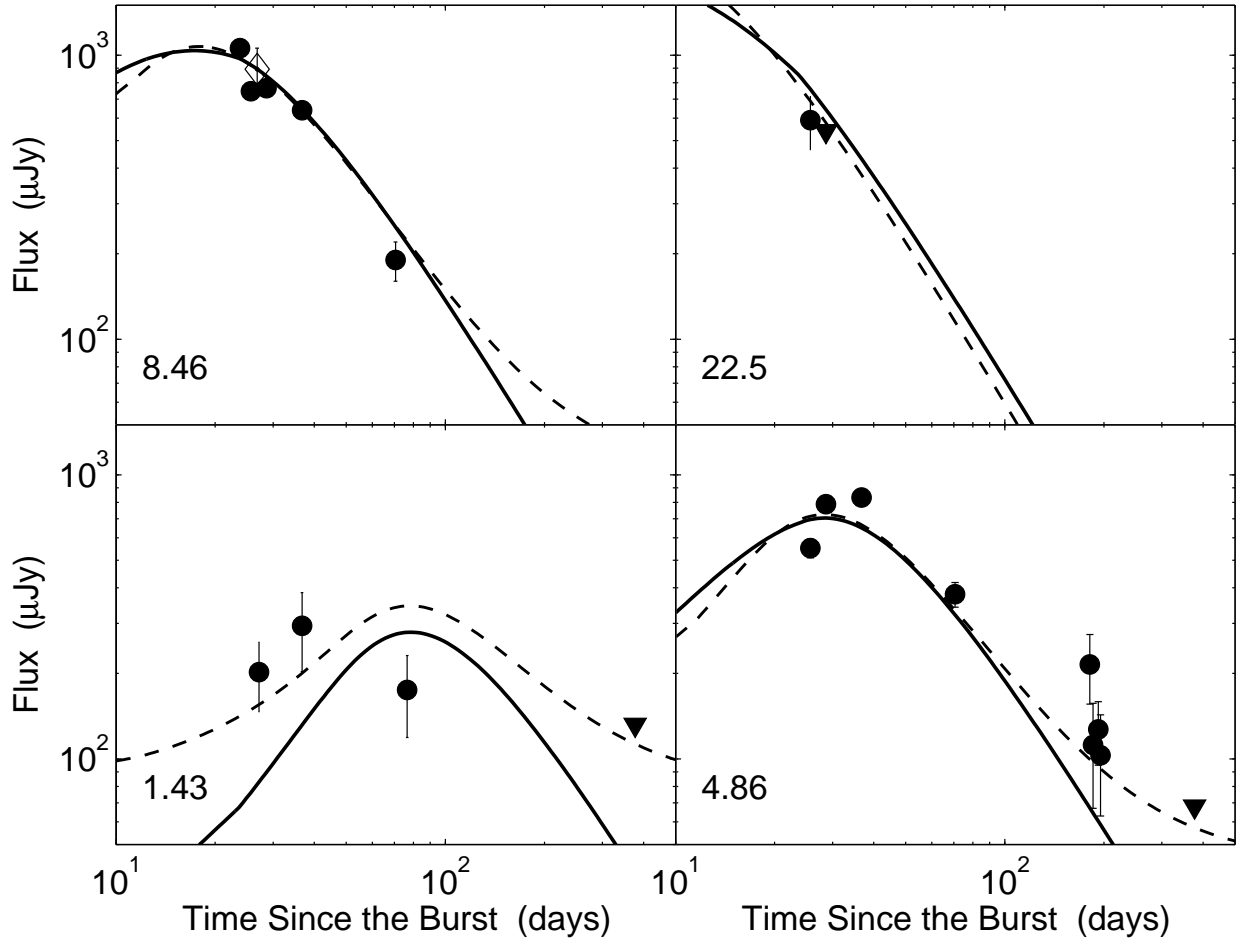


Fig. 4. We observed the field of XRF 020903 with the Very Large Array over the period $t = 25$ –370 days. A bright radio counterpart was detected at a position coincident with the optical transient. We continued monitoring the source with the VLA over the next 300 days at frequencies of 1.5, 4.9, 8.5 and 22.5 GHz. Assuming the transient source is the radio afterglow component associated with XRF 020903, we overplot the best broadband model (solid line) which predicts a total kinetic energy of 4×10^{50} erg in the afterglow. Allowing for a host galaxy emission component, we find a better fit assuming a host galaxy flux of $F_{1.4\text{GHz}} = 80$ Jy (dashed line). The implied star-formation rate from the host is $5 \text{ M}_\odot \text{ yr}^{-1}$ following the conversion from Yun & Carilli (2002). The 8.5 GHz data point marked by the open diamond symbol denotes the VLBA observation of the unresolved transient source (beam size = 1.93 × 1.73 mas).

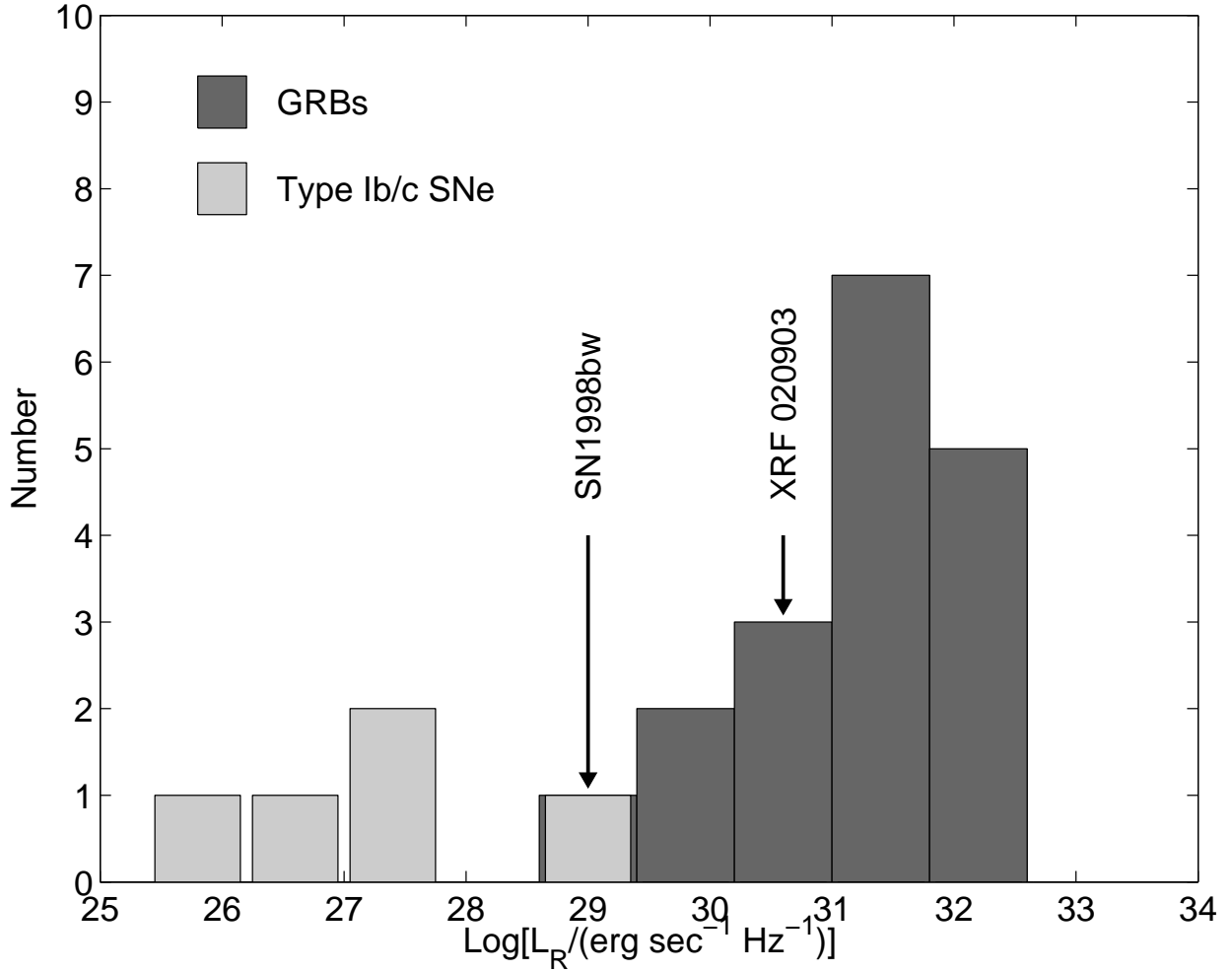


Fig. 5. The histogram above compares the peak radio luminosity for various cosmological explosions, including type Ib/c supernovae (spherical ejecta geometry) as well as typical long-duration GRBs (collimated ejecta geometry). Although the energy in the prompt emission of XRF 020903 is $10^2 - 10^3$ times lower than that observed for typical GRBs, the total kinetic energy in the afterglow of XRF 020903 is comparable to that found in typical GRBs afterglows. In comparison with a larger sample of cosmological explosions, XRF 020903 is a clear example where there is less energy coupled to high Lorentz factors.

Table 1. Optical observations of the afterglow of XRF 020903.

Date (UT)	t (days)	Telescope	R (mag)
2002 Sep 4.32	0.9	Palomar 200"	19.23 0.10
2002 Sep 10.30	6.9	Palomar 200"	20.60 0.10
2002 Sep 28.25	24.8	MDM 1.3 m	20.80 0.2
2002 Oct 7.17	33.8	Palomar 200"	20.73 0.17
2003 Jul 2.47	302.1	Palomar 200"	21.00 0.45

Table 2. Radio Observations of the afterglow of XRF 020903.

Date (UT)	t (days)	1.5 GHz (Jy)	4.9 GHz (Jy)	8.5 GHz (Jy)	22.5 GHz (Jy)
2002 Sep 27.22	23.8	1058 19	...
2002 Sep 29.11	25.7	197 70	552 42	746 37	590 125
2002 Sep 30.23 ^a	26.8	892 166	...
2002 Oct 2.06	28.6	210 91	788 45	765 41	0 270
2002 Oct 10.13	36.7	294 91	832 47	640 40	...
2002 Nov 13.02	74.0	175 56	380 38	190 30	...
2003 Mar 3.71	181.3	...	215 59
2003 Mar 7.72	185.3	...	112 45
2003 Mar 14.74	192.3	...	127 32
2003 Mar 17.69	195.3	...	103 40
2003 Sep 15.22	376.8	43 66	21 34

^aVLBA observation